

1 Journal of Biomechanics - Short Communication

2

3 **Ratio of forces during sprint acceleration: a comparison of different calculation methods**

4

5 Neil Bezodis¹, Steffi Colyer², Ryu Nagahara³, Helen Bayne⁴, Ian Bezodis⁵, Jean-Benoît Morin⁶,
6 Munenori Murata³, Pierre Samozino⁷

7

8 ¹ Applied Sports, Technology, Exercise and Medicine Research Centre, Swansea University, UK.
9 ORCID: 0000-0003-2229-3310.

10 ² Department for Health, University of Bath, UK. ORCID: 0000-0002-4973-6591.

11 ³ National Institute of Fitness and Sports in Kanoya, Japan. ORCID: 0000-0001-9101-9759
12 (Nagahara).

13 ⁴ Department of Physiology, Faculty of Health Sciences, University of Pretoria, South Africa.
14 ORCID: 0000-0002-2520-4937.

15 ⁵ Cardiff School of Sport & Health Sciences, Cardiff Metropolitan University, UK. ORCID: 0000-
16 0002-0250-032X.

17 ⁶ UJM-Saint-Etienne, Interuniversity Laboratory of Human Movement Biology, EA 7424, University
18 of Lyon, Saint-Étienne, France. ORCID: 0000-0003-3808-6762.

19 ⁷ Univ Savoie Mont Blanc, Interuniversity Laboratory of Human Movement Biology, EA 7424, F-
20 73000 Chambéry, France. ORCID: 0000-0002-1665-870X.

21

22 Corresponding author: Dr Neil Bezodis, Swansea University Bay Campus, Crymlyn Burrows,
23 Swansea, Wales, UK, SA1 8EN.

24

25 Word count: 2,147 words.

26 **Abstract**

27 The orientation of the ground reaction force (GRF) vector is a key determinant of human sprint
28 acceleration performance and has been described using ratio of forces (RF) which quantifies the ratio
29 of the antero-posterior component to the resultant GRF. Different methods have previously been used
30 to calculate step-averaged RF, and this study therefore aimed to compare the effects of three
31 calculation methods on two key “technical” ability measures: decline in ratio of forces (D_{RF}) and
32 theoretical maximal RF at null velocity (RF_0). Twenty-four male sprinters completed maximal effort
33 60 m sprints from block and standing starts on a fully instrumented track (force platforms in series).
34 RF-horizontal velocity profiles were determined from the measured GRFs over the entire acceleration
35 phase using three different calculation methods for obtaining an RF value for each step: A) the mean
36 of instantaneous RF during stance, B) the step-averaged antero-posterior component divided by the
37 step-averaged resultant GRF, C) the step-averaged antero-posterior component divided by the
38 resultant of the step-averaged antero-posterior and vertical components. Method A led to significantly
39 greater RF_0 and shallower D_{RF} slopes than Methods B and C. These differences were very large
40 (Effect size Cohen’s $d = 2.06 - 4.04$) and varied between individuals due to differences in the GRF
41 profiles, particularly during late stance as the acceleration phase progressed. Method B provides RF
42 values which most closely approximate the mechanical reality of step averaged accelerations
43 progressively approaching zero and it is recommended for future analyses although it should be
44 considered a *ratio of impulses*.

45

46 Abstract word count: 250 words.

47

48 **Keywords:** ground reaction force, impulse, sprinting, technique.

49 **Introduction**

50 The magnitude and orientation of the ground reaction force (GRF) vector is a key determinant of
51 human sprint acceleration performance. GRF orientation has been quantified by the ratio of forces
52 (RF: ratio of the antero-posterior component to the resultant GRF) as a measure of mechanical
53 effectiveness since it was first proposed by Morin et al. (2011). This provides a valuable measure of a
54 sprinter's ability to apply force in a more horizontal direction. For the same magnitude of force
55 applied by a sprinter, the horizontal change in velocity during stance – which ultimately affects
56 performance – will differ based on the orientation of the resultant GRF vector.

57

58 One prevalent use of RF data has been to establish how a sprinter's RF decreases as horizontal
59 velocity (v_H) increases across the entire acceleration phase, with this relationship well fitted by a
60 linear approximation (Morin et al., 2012; 2019; Rabita et al., 2015; Samozino et al., 2016). The
61 gradient of this linear fit is extracted as a measure of the rate of decline in ratio of forces (D_{RF}). The y-
62 intercept can be obtained as a measure of the theoretical maximal RF at null velocity (RF_0 ; Rabita et
63 al., 2015), or other measures of the relative location of this trendline are also sometimes used such as
64 the value at 0.3 s into the sprint (RF_{MAX}) to represent the RF value during the initial push-off
65 (Samozino, 2018; Samozino et al., 2016).

66

67 Whilst measures extracted from the RF- v_H trendline have been increasingly used in applied practice
68 and research (Hicks et al., 2020), the input data used to determine step-averaged RF have not been
69 consistent between studies. 'Step-averaged' is used as a descriptor throughout for ease of reading;
70 some methods can only use data during stance as there is no GRF and thus no RF during flight, whilst
71 others have previously used average forces from either just stance or the entire step but this does not
72 affect the determined RF value. For example, Morin et al. (2011, 2012) used the ratio between the
73 mean antero-posterior component and the mean resultant GRF over each contact period, Rabita et al.
74 (2015) used the mean value of the instantaneous RF over each contact period, and Samozino et al.
75 (2016) and Morin et al. (2019) used the ratio between the step-averaged antero-posterior component
76 and the resultant of the step-averaged antero-posterior and vertical components. Although

77 conceptually close, these methods are all computationally different and will not necessarily yield the
78 same value for step-averaged RF. We therefore aimed to determine the effects of calculating step-
79 averaged RF using each of the above three methods on the widely used properties of the RF- v_H
80 relationship (i.e. D_{RF} and RF_0), with a view to determining whether they can be used interchangeably
81 and, if not, to discuss the relative merits of each.

82

83

84 **Methods**

85 Following ethical approval and the provision of informed consent, 24 male sprinters (age = 20 ± 1
86 years; stature = 1.73 ± 0.06 m; mass = 65.7 ± 4.0 kg; 100 m personal best = 11.26 ± 0.39 s) completed
87 two maximal effort 60 m indoor sprints from a standing start and two from starting blocks. All
88 sprinters wore their own spiked shoes and used their preferred block settings. A 52-m series of force
89 platforms (TF-3055, TF-32120, TF-90100, Tec Gihan, Uji, Japan) was located under the track from
90 which raw GRF data were collected at 1000 Hz. The start of data capture was synchronised with the
91 starting signal and data capture was manually stopped after the sprinter had run 52 m. Standing and
92 block starts were included because both are used by track sprinters at different phases within the
93 season but the determination of these performance metrics (e.g. D_{RF} , RF_0) often happens year-round.
94 These metrics are also widely used in team sports athletes who start from standing, and thus the
95 separate consideration of effects for both starting conditions yields greater value to the applied
96 community.

97

98 The vertical and antero-posterior components of the GRF data were low-pass filtered at 70 Hz, and
99 instantaneous horizontal velocity was determined using the impulse-momentum relationship
100 accounting for the influence of air resistance (Samozino et al., 2016; Colyer et al., 2018).

101 Instantaneous RF was determined from the antero-posterior and vertical components of the filtered
102 GRF data as the ratio of the antero-posterior component to the 2D resultant. Given our aim, the two-
103 dimensional (sagittal plane) representation of the GRF vector was used to be consistent with the
104 previous studies which have determined RF in sprinting, and the effects of including the medio-lateral

105 component in the resultant magnitude are negligible (Rabita et al., 2015). Movement onset was
106 identified from the raw antero-posterior GRF using a two standard deviation threshold for the block
107 starts. The same procedure was initially applied to the standing starts but because of considerable
108 variation in the standing start technique between sprinters, visual identification by an experienced
109 analyst was used for all standing start trials so that minor fluctuations associated with preparatory
110 movements were ignored and the first clear and sustained increase in force was identified. All
111 subsequent touchdown and toe-off events were identified using a 25 N threshold in the vertical GRF
112 data.

113

114 Step-averaged RF was determined from the block exit/initial push-off step to the final step on the
115 force platforms using each of three different methods in line with this study's aims:

116

- 117 A. The mean value of instantaneous RF over the whole stance phase (Rabita et al., 2015).
- 118 B. The step-averaged antero-posterior component divided by the step-averaged resultant (2D
119 sagittal) GRF (Morin et al., 2011; 2012).
- 120 C. The step-averaged antero-posterior component divided by the resultant of the step-averaged
121 antero-posterior and vertical components (Samozino et al., 2016; Morin et al., 2019).

122

123 To determine the relationships between RF and v_H for each of the above three methods, average v_H
124 from the corresponding time interval was used. For method A, v_H was averaged over just the stance
125 phase, whereas for methods B and C v_H was determined from touchdown to the next touchdown (this
126 was done to enable a direct comparison between methods B and C and had only a minor influence on
127 the v_H values between these and Method A, and therefore on the outcome of this study, see Figure 1).
128 For each of the three methods, linear trendlines were fitted over the entire acceleration phase from the
129 initial block exit/push-off to the step with the highest velocity (mean \pm SD = step 24 ± 2 for block
130 starts; step 23 ± 2 for standing starts), and D_{RF} and RF_0 were extracted.

131

132 Mean values of the two trials for each sprinter in each condition (standing, blocks) were calculated.
133 Twelve standing start trials (across nine sprinters) were rejected because the sprinter was deemed not
134 stationary at the start signal and thus $n = 21$ for the standing start condition (values from one
135 successful trial were used for six sprinters). D_{RF} and RF_0 were compared between the three methods
136 using a repeated-measures ANOVA with Bonferroni post hoc tests (alpha level = 0.05), and the
137 systematic bias and random errors were quantified using a Bland-Altman analysis. Cohen's effect
138 sizes (d) were used to describe the magnitude of the pairwise systematic bias based on the thresholds
139 proposed by Hopkins et al. (2009) of 0.2, 0.6, 1.2 and 2.0 for small, moderate, large and very large,
140 respectively.

141 **Results**

142 For both block and standing starts, there was a significant main effect of calculation method on D_{RF}
143 and RF_0 , with post-hoc tests revealing all three calculation methods yielded different values from one
144 another for all comparisons (Table 1). The method using the mean of the instantaneous RF data (i.e.
145 Method A) always had a lower RF_0 and a shallower D_{RF} than methods B and C (Table 1, Figure 1).

146

147 ****Figure 1 near here****

148

149 The random differences (i.e. 95% limits of agreement) were always larger for Method C compared
150 with Method A than for Method B compared with Method A (Figure 2; Table 2). All effect size
151 differences for comparisons with Method A were very large, whilst the effect size differences between
152 Methods B and C ranged from trivial to moderate (Table 2).

153 **Table 1.** Theoretical maximal RF at null velocity (RF_0) and rate of decline in RF (D_{RF}) for block starts and standing starts determined from the linear fit to
 154 ratio of forces (RF) and horizontal velocity data using step-averaged RF data from each of the three different calculation methods (mean \pm SD).
 155

	Method A: using step-averaged RF determined as the mean of the instantaneous RF data	Method B: using step- averaged RF determined from step- averaged A-P GRF and step-averaged resultant GRF	Method C: using step- averaged RF determined from step- averaged A-P GRF and step-averaged vertical GRF	ANOVA results
Block starts				
RF_0 (%)	64.70 \pm 2.69 ^{B,C}	72.01 \pm 3.01 ^{A,C}	73.94 \pm 3.15 ^{A,B}	F(2,46) = 616.180, $\eta^2_{partial} = 0.964$, p<0.001
D_{RF} (%·s/m)	-5.64 \pm 0.45 ^{B,C}	-7.21 \pm 0.44 ^{A,C}	-7.38 \pm 0.45 ^{A,B}	F(2,46) = 1372.107, $\eta^2_{partial} = 0.984$, p<0.001
Standing starts				
RF_0 (%)	63.71 \pm 3.58 ^{B,C}	71.20 \pm 3.67 ^{A,C}	72.28 \pm 3.71 ^{A,B}	F(2,40) = 295.925, $\eta^2_{partial} = 0.937$, p<0.001
D_{RF} (%·s/m)	-5.44 \pm 0.42 ^{B,C}	-7.06 \pm 0.42 ^{A,C}	-7.13 \pm 0.42 ^{A,B}	F(2,40) = 662.767, $\eta^2_{partial} = 0.971$, p<0.001

156 Note: superscript A, B, C = significantly different (all p < 0.001) from method A, B or C, respectively, in pairwise post-hoc comparisons with Bonferroni adjustment.
 157

158 **Table 2.** Systematic bias \pm 95% limits of agreement (and Cohen's d effect size) for each pairwise
 159 comparison of methods for both RF_0 and D_{RF} from block starts and standing starts.
 160

RF_0 (%) – block starts		
	Method B	Method C
Method A	7.30 ± 3.01 (d = 2.56)	9.23 ± 3.39 (d = 3.15)
Method B	-	1.93 ± 0.84 (d = 0.63)

RF_0 (%) – standing starts		
	Method B	Method C
Method A	7.48 ± 4.02 (d = 2.06)	8.57 ± 4.36 (d = 2.35)
Method B	-	1.08 ± 0.58 (d = 0.29)

D_{RF} (%·s/m) – block starts		
	Method B	Method C
Method A	-1.57 ± 0.41 (d = 3.53)	-1.74 ± 0.45 (d = 3.86)
Method B	-	-0.17 ± 0.09 (d = 0.39)

D_{RF} (%·s/m) – standing starts		
	Method B	Method C
Method A	-1.62 ± 0.56 (d = 3.89)	-1.70 ± 0.59 (d = 4.04)
Method B	-	-0.08 ± 0.06 (d = 0.18)

161

162 ****Figure 2 near here****

163

164

165 **Discussion**

166 The method used to determine step-averaged RF has a significant effect on the determined D_{RF} and
167 RF_0 measures. There is a systematic component to these differences, with Method yielding lower RF_0
168 and shallower D_{RF} measures than Methods B and C for all trials from both types of start (Figure
169 2a,b,d,e). These differences were very large based on the effect sizes, and their magnitude should be
170 considered important in the context of typical between-participant variation (Haugen et al., 2019) or
171 within-participant change in response to training (Lahti et al., 2020). Method B always had a lower
172 RF_0 and a shallower D_{RF} than Method C, although these differences were considerably smaller than
173 those compared with Method A, ranging from trivial to moderate (Figure 2c,f). In addition to these
174 systematic effects, there were also considerable random differences as illustrated by the 95% limits of
175 agreement (Figure 2). These demonstrate that the magnitude of the differences between the three
176 methods varies from one sprinter to the next, and thus a simple systematic offset to convert between
177 methods is not appropriate.

178

179 The systematic differences in D_{RF} and RF_0 between Method A and the other two methods primarily
180 occur because of differences in the sequence of calculations (i.e. when values are squared and
181 averaged). Individual differences in the shape of the GRF profiles produced during stance and the
182 consequent effects on the instantaneous RF profile explain the random differences, particularly during
183 late stance when GRF magnitudes are relatively low and RF can reach high values (Figure 3). Given
184 the nature of the calculations used in Method A, the instantaneous RF values during late stance have
185 an equal weighting to all other timepoints despite occurring when the GRF is less “functionally
186 effective” due to it already being low and decreasing further. The effects of this on step-averaged RF
187 become increasingly more pronounced as the acceleration phase progresses (Figure 1). This may be
188 due to the average RF being higher up to around mid-stance during early acceleration than mid-
189 acceleration (i.e. step 1 vs. step 13; Figure 3) or because the rate of decline in the horizontal GRF
190 component during late stance becomes relatively lower than that of the vertical component as the
191 acceleration phase progresses (i.e. step 13 vs. step 1; Figure 3), potentially because of the changing
192 late stance kinematics with the trunk more upright and the hip more extended later in the acceleration

193 phase (Schache et al., 2019). Method A is the most mathematically appropriate as a direct measure of
194 mean RF. However, step averaged accelerations are further from zero than Methods B and C at the
195 end of the acceleration phase, and thus its applied mechanical meaning is less clear.

196

197 ****Figure 3 near here****

198

199 Although the differences between Methods B and C were only trivial to moderate, they yielded
200 different outputs from each other because of differences in the calculation approach. Method C should
201 not be used when GRFs are available because mean horizontal force and mean vertical force should
202 not be used to determine mean resultant force. However, this is the only computation method possible
203 when using simple modelled values from a macroscopic approach (Samozino et al., 2016; Morin et
204 al., 2019) and it therefore provides a viable alternative for field-based assessment given the magnitude
205 of the differences reported.

206

207 Method B is a *ratio of impulses* rather than a ratio of forces. This method provides values closer to the
208 mechanical reality of step averaged accelerations approaching zero (aside from air resistance effects)
209 at the end of the acceleration phase. Method B therefore provides a more appropriate assessment of
210 “mechanical effectiveness” over an entire step than Method A as it is not overly affected by nuances
211 in the GRF profile during late stance when force production is low, particularly later in the
212 acceleration phase. Instantaneous RF data, as used in Method A, may still provide valuable
213 information when within-stance technique is of interest (e.g. Bezodis et al., 2019; Colyer et al., 2018)
214 but caution should be applied to over-interpretation of RF values when GRF magnitudes are low.

215

216 The method used to determine step-averaged RF affects the determination of measures related to
217 “mechanical effectiveness” in sprinting. Researchers and coaches must apply caution to the
218 interpretation and comparison of results depending on which calculation method was employed.

219 Using instantaneous RF data (Method A) leads to step-averaged RF values which are further from
220 mechanical reality as a sprint progresses, but instantaneous RF data may be useful when focusing on

221 within-stance technique. The resultant of the step-averaged antero-posterior and vertical components
222 should only be used as the denominator (Method C) in simple macroscopic models when GRF data
223 are unavailable. The use of step-averaged antero-posterior and resultant (2D) force magnitudes
224 (Method B) is recommended to assess “mechanical effectiveness” in sprinting as this provides data
225 closer to the mechanical reality, but these data are a *ratio of impulses* due to the nature of their
226 calculation.

227

228

229 **Conflict of interest statement**

230 None of the authors have any financial or personal relationships with other people or organisations
231 that could inappropriately influence this work.

232

233

234 **References**

235 Bezodis, N. E., Walton, S. P., & Nagahara, R. (2019). Understanding the track and field sprint start
236 through a functional analysis of the external force features which contribute to higher levels of
237 block phase performance. *Journal of Sports Sciences*, 37(5), 560-567.

238 Colyer, S. L., Nagahara, R. & Salo, A. I. T. (2018). Kinetic demands of sprinting shift across the
239 acceleration phase: novel analysis of entire force waveforms. *Scandinavian Journal of*
240 *Medicine and Science in Sports*, 28(7), 1784-1792.

241 Haugen, T. A., Breitschädel, F., & Seiler, S. (2019). Sprint mechanical variables in elite athletes: Are
242 force-velocity profiles sport specific or individual? *PLoS ONE*, 14(7), e0215551.

243 Hicks, D. S., Schuster, J. G., Samozino, P., & Morin, J.-B. (2020). Improving mechanical
244 effectiveness during sprint acceleration: practical recommendations and guidelines. *Strength*
245 *and Conditioning Journal*, 42(2), 45-62.

246 Hopkins, W. G., Marshall, S. W., Batterham, A. M., & Hanin, J. (2009). Progressive statistics for
247 studies in sports medicine and exercise science. *Medicine & Science in Sports & Exercise*,
248 *41*(1), 3–13.

249 Lahti, J., Jiménez-Reyes, P., Cross, M. R., Samozino, P., Chassaing, P., Simond-Cote, B., Ahtiainen,
250 J. P., & Morin, J.-B. (2020). Individual sprint force-velocity profile adaptations to in-season
251 assisted and resisted velocity-based training in professional rugby. *Sports*, *8*(5), 74.

252 Morin, J.-B., Edouard, P., & Samozino, P. (2011). Technical ability of force application as a determinant
253 factor of sprint performance. *Medicine & Science in Sports & Exercise*, *43*(9), 1680-1688.

254 Morin, J.-B., Bourdin, M., Edouard, P., Peyrot, N., Samozino, P. & Lacour, J.-R. (2012). Mechanical
255 determinants of 100-m sprint running performance. *European Journal of Applied Physiology*,
256 *112*(11), 3921-3930.

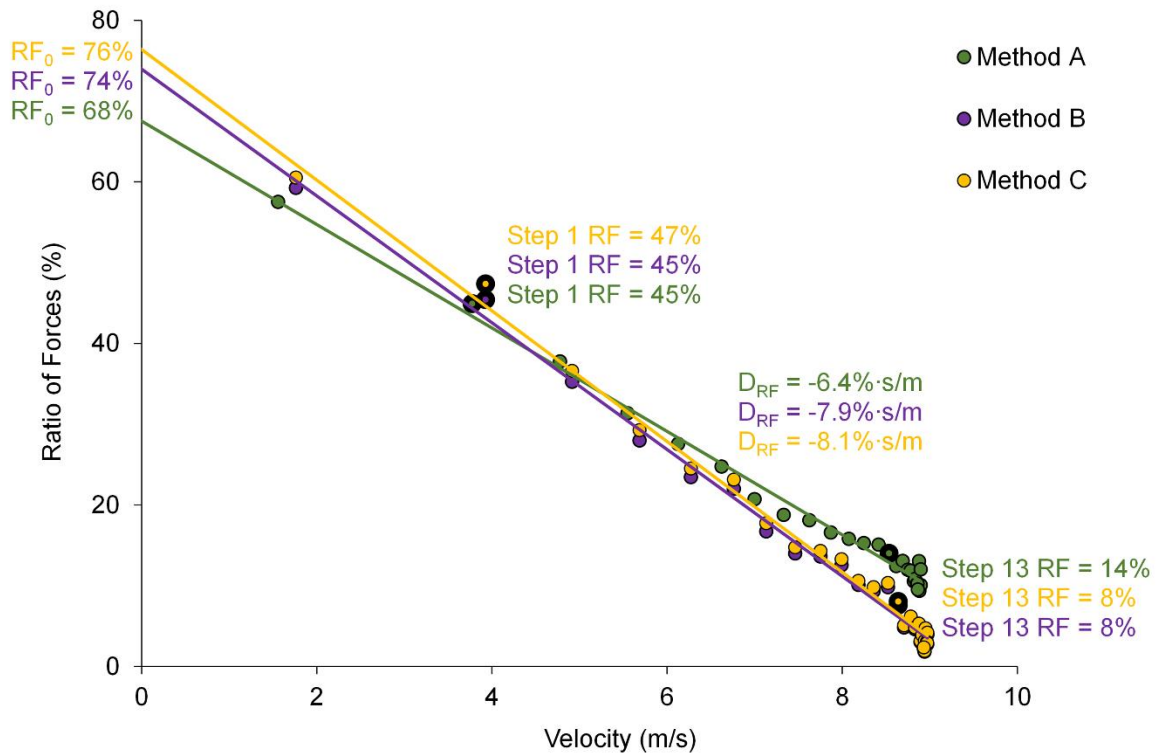
257 Morin, J.-B., Samozino, P., Murata, M., Cross, M. R. & Nagahara, R. (2019). A simple method for
258 computing sprint acceleration kinetics from running velocity data: replication study with
259 improved design. *Journal of Biomechanics*, *94*, 82-87.

260 Rabita, G., Dorel, S., Slawinski, J., Saez-de-Villarreal, E., Couturier, A., Samozino, P. & Morin J.-B.
261 (2015). Sprint mechanics in world-class athletes: a new insight into the limits of human
262 locomotion. *Scandinavian Journal of Medicine and Science in Sports*, *25*(5), 583-594.

263 Samozino, P. (2018). A simple method for measuring force, velocity and power capabilities and
264 mechanical effectiveness during sprint running. In J.-B. Morin & P. Samozino (Eds),
265 *Biomechanics of Training and Testing* (pp. 237-267). Cham, Switzerland: Springer
266 International Publishing.

267 Samozino, P., Rabita, G., Dorel, S., Slawinski, J., Peyrot, N., Saez de Villarreal, E. & Morin, J.-B.
268 (2016). A simple method for measuring power, force, velocity properties, and mechanical
269 effectiveness in sprint running. *Scandinavian Journal of Medicine and Science in Sports*, *26*(6),
270 648-658.

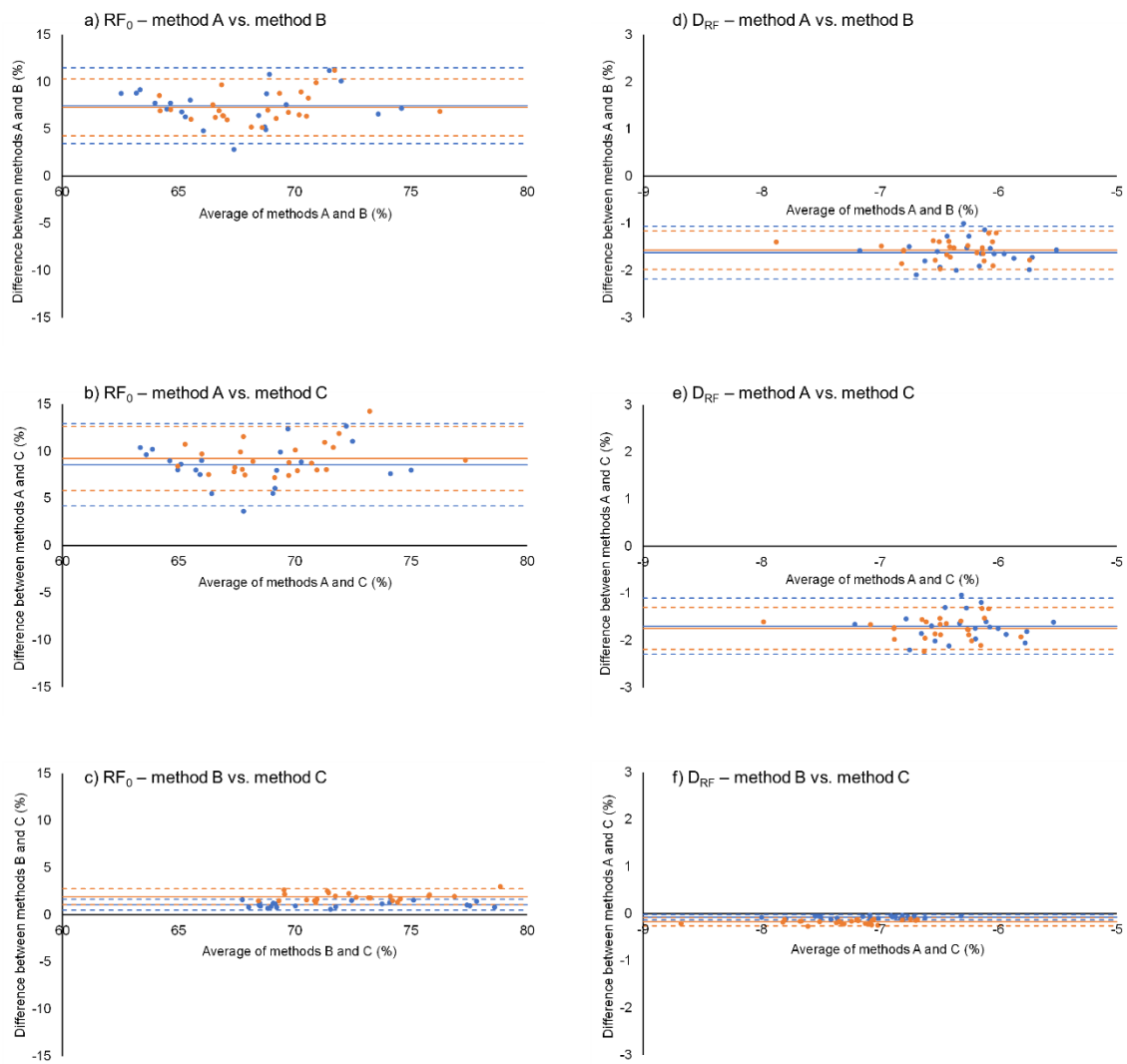
271 Schache, A. G., Lai, A. K. M., Brown, N. A. T., Crossley, K. M. & Pandy, M. G. (2019). Lower-limb
272 joint mechanics during maximum acceleration sprinting. *Journal of Experimental Biology*,
273 222(22), jeb209460.



274

275 **Figure 1.** Ratio of forces-horizontal velocity relationships compared between the three calculation
 276 methods for a typical trial from blocks for one participant. These relationships are fitted to all data
 277 from the initial block exit/push-off to the step with the highest average horizontal velocity. The stated
 278 step 1 and step 13 step-averaged RF values correspond to the respective data points with a bold
 279 outline (note: for step 13 the values for methods B and C are very close). These bold data points
 280 correspond to the continuous GRF data in Figure 3 which illustrate reasons for the differences
 281 between the methods as the acceleration phase progresses.

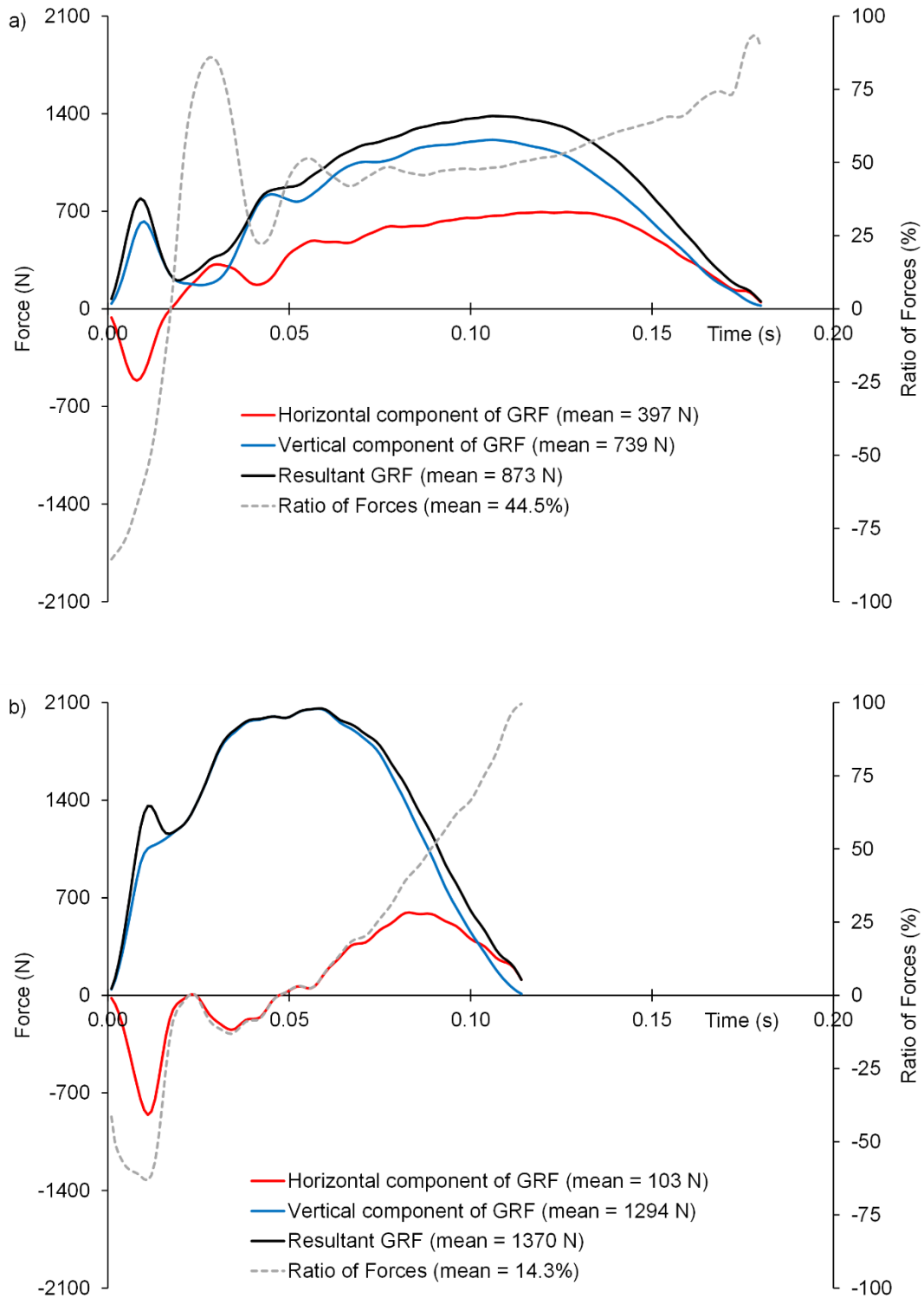
282



283

284 **Figure 2.** Bland-Altman plots for RF_0 and D_{RF} between each pairwise comparison of the three
 285 methods. Block start trials are shown in orange and standing start trials are shown in blue. All axes are
 286 scaled the same for each variable for ease of comparison between figures.

287



288

289 **Figure 3.** Vertical and horizontal components of the ground reaction force, resultant ground reaction
 290 force (2D sagittal), and instantaneous ratio of forces (plotted on secondary y-axis) during a) step 1 and
 291 b) step 13 for a typical trial from blocks. Note: this is the same trial as the data presented in Figure 1
 292 (in which data points corresponding to steps 1 and 13 are identified with a bold outline).